

Heat capacity measurements of sub-nanoliter volumes of liquids using bimaterial microchannel cantilevers

M. F. Khan,^{1,2} N. Miriyala,^{1,2} J. Lee,^{2,3} M. Hassanpourfard,^{1,2} A. Kumar,⁴ and T. Thundat^{1,2}

¹*Ingenuity Lab, Edmonton, Alberta T6G 2R3, Canada*

²*Department of Chemical and Materials Engineering, University of Alberta, Edmonton, Alberta T6G 2R3, Canada*

³*Department of Mechanical Engineering, Sogang University, 121-742 Seoul, South Korea*

⁴*Department of Mechanical Engineering, University of Alberta, Edmonton, Alberta T6G 2R3, Canada*

(Received 7 February 2016; accepted 10 May 2016; published online 25 May 2016)

Lab-on-a-Chip compatible techniques for thermal characterization of miniaturized volumes of liquid analytes are necessary in applications such as protein blotting, DNA melting, and drug development, where samples are either rare or volume-limited. We developed a closed-chamber calorimeter based on a bimaterial microchannel cantilever (BMC) for sub-nanoliter level thermal analysis. When the liquid-filled BMC is irradiated with infrared (IR) light at a specific wavelength, the IR absorption by the liquid analyte results in localized heat generation and the subsequent deflection of the BMC, due to a thermal expansion mismatch between the constituent materials. The time constant of the deflection, which is dependent upon the heat capacity of the liquid analyte, can be directly measured by recording the time-dependent bending of the BMC. We have used the BMC to quantitatively measure the heat capacity of five volatile organic compounds. With a deflection noise level of ~ 10 nm and a signal-to-noise ratio of 68:1, the BMC offers a sensitivity of 30.5 ms/(J g⁻¹ K⁻¹) and a resolution of 23 mJ/(g K) for ~ 150 pl liquid for heat capacity measurements. This technique can be used for small-scale thermal characterization of different chemical and biological samples. *Published by AIP Publishing.* [<http://dx.doi.org/10.1063/1.4952614>]

Sensitive real-time techniques for thermal characterization of liquid analytes are needed in Lab-on-a-Chip platforms.^{1,2} Some key application requirements include DNA melting,³ study of protein folding,⁴ and biochemical characterization,⁵ where it is challenging to employ existing bench-top characterization techniques due to expensive or limited amounts of samples. Among many thermal characteristics of a liquid sample, precise knowledge of heat capacity is crucial for thermodynamic analysis of processes such as conformational changes⁶ and phase transitions.⁷ For these applications, many chip scale thermal analysis systems such as micro-calorimeters have been developed with different configurations.⁸ One example is a protein analysis platform where western blots are being implemented at chip scale.⁹ In general, micro-calorimeters can be categorized in two groups based on the heating method: resistive heating and optical heating. Many researchers have reported resistively heated calorimeters such as suspended calorimeters with picowatt resolution^{10,11} and cantilever-based calorimeters, used for simultaneous temperature and mass sensing.¹² While resistive heating techniques offer precisely controlled heating, they generally require complicated fabrication. Nanomechanical torsional resonators,¹³ bimaterial cantilevers,^{14–16} and carbon nanotubes¹⁷ have been demonstrated as miniature calorimeters using optical heating. Such platforms offer high sensitivity as well as simple fabrication methods, but exhibit a limited ability to characterize liquid samples that require extra components for sample loading and handling. Efforts towards developing chip-scale thermal characterization of liquid samples include fabrication of closed-chamber calorimeters^{18–22} and open-chamber calorimeters.^{23–25} Though closed-chamber calorimeters have higher thermal loss,

they are more desirable for online real-time analysis of an analyte.

Closed-chamber calorimeters (with resistive heating capacity) can perform calorimetry for small amounts of liquid samples with high resolution, but they suffer from challenges such as the presence of resistive heaters, material selection, and sample volumes. To overcome the challenges of thermal analysis of picoliter volumes of liquids, we have developed an optically heated closed-chamber calorimeter. Here, we present a bimaterial microchannel cantilever (BMC) to determine the heat capacity of five different volatile organic compounds (VOCs), with varying heat capacity. The BMC was originally developed for deflection-based optical spectroscopy,²⁶ inertial mass sensing,²⁷ and viscosity measurements.²⁸ We have used these BMCs for the calorimetric characterization of liquids as they offer a convenient method for the thermal characterization of sub-nanoliters of liquid reagents. A sample analyte (in the BMC) is heated by exposing the BMC to a selected optical wavelength, and its thermal properties are measured using mechanical responses of the cantilever. The time constant (calculated from the BMC's thermal response) is three orders of magnitude lower than previously reported sensors for heat capacity measurements^{18,29,30} which enables fast online measurements in a batch format. Additionally, the structural material (silicon nitride, SiN) provides low thermal conductivity and high structural rigidity, which are desirable for retaining heat for relatively longer time periods.

We have fabricated the BMC with dimensions of 76 μ m width, 600 μ m length, and 1 μ m in thickness (t_1), with a 3 μ m high microfluidic channel on one side (top) (Figs. 1(a) and 1(b)). The internal volume of the channel is approximately

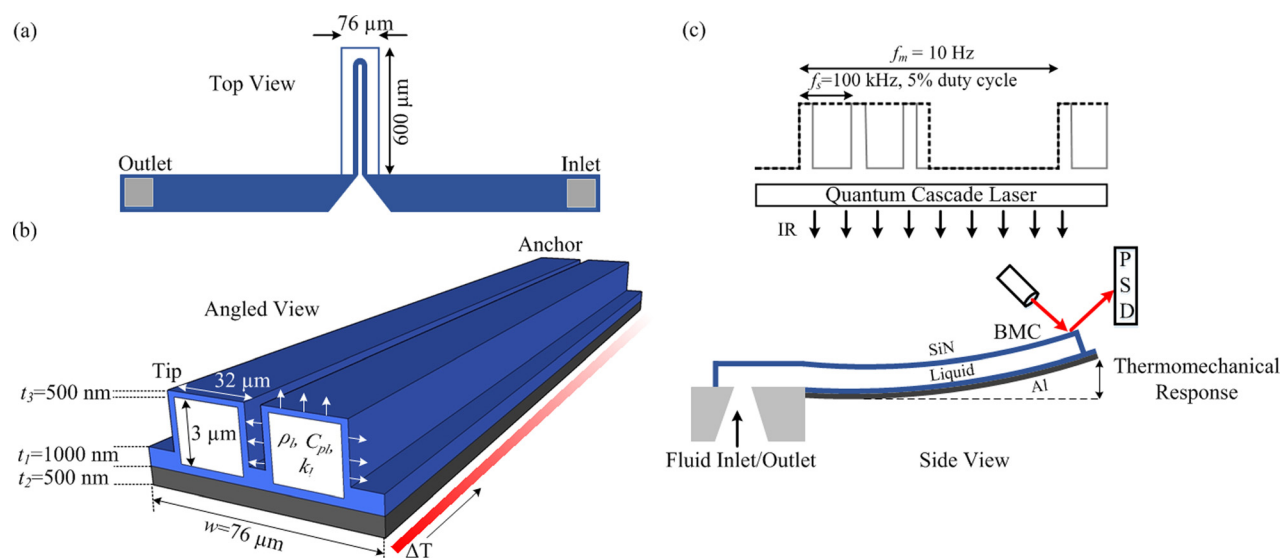


FIG. 1. (a) Schematic of top view of the BMC. (b) Cross section of the BMC with aluminium (Al) and silicon nitride (SiN) layers. (c) Schematic of the experimental setup where a PSD is used to measure the deflection (thermomechanical response) and resonance frequency of the BMC. IR light is provided from top of the cantilever while liquid is supplied from the bottom of the substrate which is supporting the BMC.

150 pl. The spring constant of the BMC is ~ 0.03 N/m. The cantilever is turned into a bimetallic structure by depositing aluminium (on the bottom) with an optimized thickness (t_2) of 500 nm. The fabrication details of the BMC are published elsewhere.^{26,31} In order to heat the liquid inside the BMC, it is irradiated with infrared (IR) light from a tunable quantum cascade laser (QCL) (Day Light Solution, USA) with an optical power of 86 mW at 985 cm^{-1} . The QCL is operated in a pulsed mode with a switching frequency (f_s) of 100 kHz and a duty cycle of 5%. The beam diameter of the laser spot is approximately 2.5 mm, which illuminates the entire BMC and ensures uniform light absorption and heat generation. When the liquid inside the BMC absorbs the light, localized heat is generated due to non-radiative decay. The BMC deflects upwards (i.e., towards the side opposite to the metal layer) due to a mismatch in the thermal expansion of SiN and Al (Fig. 1(c)).

The BMC deflection is proportional to multiple factors, such as the thermomechanical sensitivity of the device, the optical intensity, the irradiation time, the light absorption coefficient of a sample inside the microchannel, the thermal properties of the sample, and the difference of the thermal expansion coefficient of the BMC materials. To maximize the deflection of the BMC, it is very important to irradiate a reagent inside the BMC for time duration equal to or higher than its time constant (around 10 ms). Therefore, in this study, in order to get its steady state thermomechanical responses, IR light is modulated at a frequency (f_m) of 10 Hz,³² providing an irradiation time of 50 ms.

Before introducing a liquid sample, thermal characterization of the empty BMC (with ambient air) is carried out which serves as a reference signal. The air-filled BMC is irradiated with IR light for 50 ms (see Fig. 2(a)). During the ON-cycle, the SiN in the BMC absorbs IR radiation (as shown in Fig. S3 in the supplementary material³³) and localized heat is generated in the BMC structure which deflects the BMC. The maximum deflection (thermomechanical response) of the BMC is recorded as $2.42\text{ }\mu\text{m}$. After a steady

deflection for 16 ms, the BMC goes to an equilibrium deflection position determined by thermal conductivity and stiffness of the whole structure. Since the experiment is performed at room temperature and atmospheric pressure, there is a convective heat loss through the SiN and Al layers.

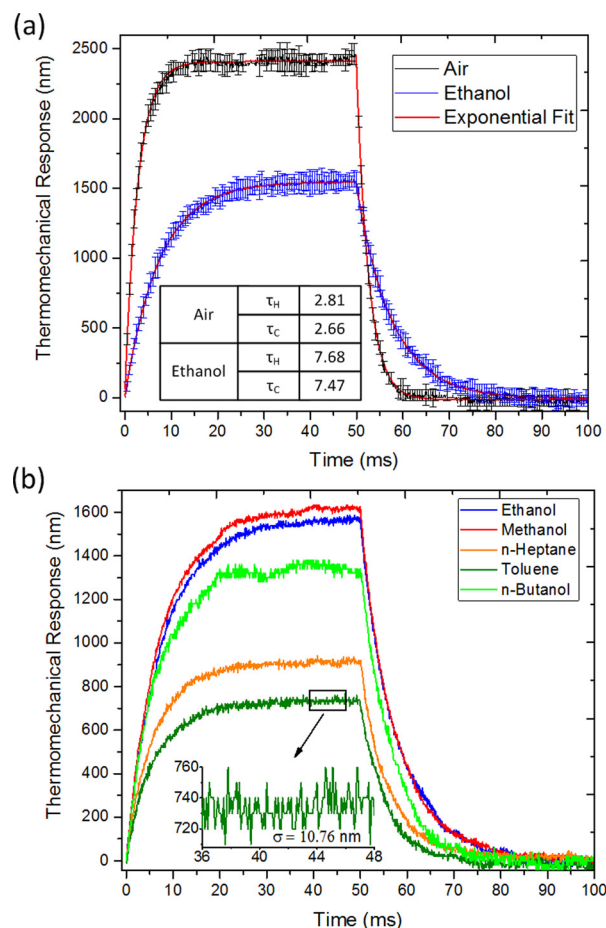


FIG. 2. (a) Thermomechanical response of the BMC filled with ambient air and ethanol. (b) Thermomechanical response of the BMC filled with five different VOCs (ethanol, methanol, n-heptane, toluene, and n-butanol).

Once the IR light is turned off, the BMC relaxes back to its original position. The relaxation time depends on the rate of conductive and convective heat loss through the anchor and suspended body of the BMC, respectively. The time constants, τ_H (for heating) and τ_C (cooling), are calculated by fitting the data with an exponential decay/growth function (see Fig. S1 in the supplementary material³³). The average value of τ_H and τ_C is calculated as 2.81 ± 0.08 ms and 2.66 ± 0.16 ms, respectively. In order to ensure reproducibility, the experiments were performed on two different chips with similar BMCs. The measurements for the second BMC are presented in Fig. S2 in the supplementary material.³³

After characterization with air, the BMC is filled with 99.9% pure ethanol and irradiated with IR light. Ethanol is considered as a reference VOC sample since it is one of the most commonly used solvents in various life science studies. Depending on its heat capacity, the $3 \mu\text{m}$ thick layer of ethanol stores some of the heat while the surplus heat is transferred to Al layer. Unlike SiN, ethanol does not absorb considerable IR at this wavelength. When compared to the BMC filled with air, it takes a longer time (38 ms) for the cantilever to reach a saturation amplitude of $1.54 \mu\text{m}$. The deflection amplitude is approximately 36% lower than that of the air-filled BMC. This is likely due to ethanol's higher thermal conductivity which increases heat dissipation. As shown in the table (Fig. 2(a)), the BMC filled with ethanol exhibits a τ_H of 7.68 ± 0.36 ms and a τ_C of 7.47 ± 0.49 ms which are significantly higher than the time constants of the BMC filled with air. When comparing the air- and ethanol-filled BMCs, the large difference in their time constants can be attributed to the difference in their thermal masses. As liquids can be differentiated by their thermal properties, the liquid inside the BMC can be differentiated by the thermomechanical response of the BMC. This method can help in determining the heat capacities of a large range of sub-nanoliter volumes of liquids.

In order to measure the heat capacity of VOCs, the BMC is loaded with five different liquid solutions; methanol, ethanol, n-heptane, toluene, and n-butanol. These chemicals have negligible IR absorption at a wavenumber of 985 cm^{-1} . Fig. 2(b) presents the thermomechanical response of the BMC filled with the five different solutions. It is evident that the BMC exhibits different responses (time constant and deflection amplitude) with different solutions due to their different thermal mass and heat transfer characteristics. The thermal time constant, $\tau = RC = (L/kA)(\rho C_p V)$, mainly depends on the collective thermal conductivity (k), heat capacity (C_p), and density (ρ) of the sample-filled BMC since the length (L), cross-sectional area (A), and volume (V) are fixed for a given BMC. The effect of the thermal properties of each material can be calculated by mass-weighted average value, where the liquid sample, SiN, and Al constitute 8.53%–10.6%, 81.21%–84.76%, and 6.43%–6.71% mass of the BMC, respectively. With these proportions, the thermal conductivity and density of all tested liquids are smaller than those of SiN and Al by two orders of magnitude. Therefore, the time constant of the sample-filled BMC is not sensitive to these two parameters of the liquids. However, the heat capacity of the liquids is comparable to that of SiN and higher than that of Al by two orders of magnitude.

Therefore, the heat capacity of a liquid present in the BMC plays a dominant role in determining the temporal thermo-mechanical responses of the BMC. For example, with the BMC filled with methanol, the average time constant (heating and cooling) is measured to be 7.85 ± 0.45 ms which corresponds to the mass-weighted average of the heat capacity (C_{pm}) of methanol, SiN and Al as 0.24, 0.58, and 0.06 J/(g K) , respectively. The inset in Fig. 2(b) shows a magnified view of the steady state deflection of the BMC filled with toluene, where the steady state noise level of the quasi-static deflection is measured to be 10.76 nm . For all tested liquid samples, the noise and signal-to-noise ratio (SNR) range from 10.76 nm to 21.6 nm , and from 68:1 to 78:1, respectively.

In order to calculate the mass-weighted average of the heat capacity of the solutions, their mass is calculated from a known volume (V) of the microchannel and density (ρ_l) of each solution. Due to fabrication tolerances, the microchannel volume can differ by 6% among different BMCs from the same batch. As the BMC operates in a quasi-static mode, its resonance frequency (f_r) is also measured while measuring static deflection. With an air-filled BMC, f_r is recorded as $16.692 \pm 0.02 \text{ kHz}$ from twenty measurements. The standard deviation of the resonance frequency (SD_{f_r}) of the liquid-filled BMC is calculated to be 18 Hz from twenty measurements. The density of the solutions is extracted from the frequency shifts.³¹ Fig. 3(a) presents a plot on resonance frequency vs. density of the liquid samples for the BMC. The sensitivity ($S_\rho = f_r/\rho$) and resolution ($R_\rho = SD_{f_r}/S_\rho$) for density measurements are calculated to be 2.8 Hz/kg m^{-3} and 6.4 kg m^{-3} , respectively. After each solution, the BMC is emptied, washed, with deionized water and dried with dry air. Its resonance frequency is measured and matched with $f_r = 16.692 \text{ kHz}$ with variations of less than 0.1%. This ensures cleanliness of the BMC channel.

With known volumes of SiN, Al, and liquid sample, the information on density helps in calculating mass proportions of each material. This further helps to calculate the weighted average heat capacity (responsible for thermal response of the BMC) of each material of the BMC. With mass ratios (m_R) ranging from 8.53% (n-heptane) to 10.6% (toluene), the weighted average heat capacity for methanol, ethanol, n-heptane, toluene, and n-butanol are calculated to be 0.24, 0.23, 0.21, 0.18, and 0.2 J/(g K) , respectively. The average of the weighted heat capacity of SiN and Al are calculated to be 0.57 and 0.06 J/(g K) , respectively.

Fig. 3(b) shows the relationship between the mass-weighted average heat capacity (C_{pm}) of the liquid samples and the time constant of the BMC. From the slope, the average sensitivity ($S_C = \tau/C_{pm}$) is calculated to be $30.5 \text{ ms/(J g}^{-1} \text{ K}^{-1})$. From the error bars (in the time constant) and the slope, average resolution in the heat capacity is calculated as 23 mJ/(g K) . For samples having heat capacities in a similar range, this data can be used as a calibration for measuring real values of heat capacities (C_{pl}) of unknown samples. In order to determine C_{pl} of an unknown sample, the required parameters include known volume (V) of each material (SiN, Al, and liquid), measured density (ρ_l), measured time constant (τ), and measurement sensitivity (S_C). The following relationship is used to calculate C_{pl} :

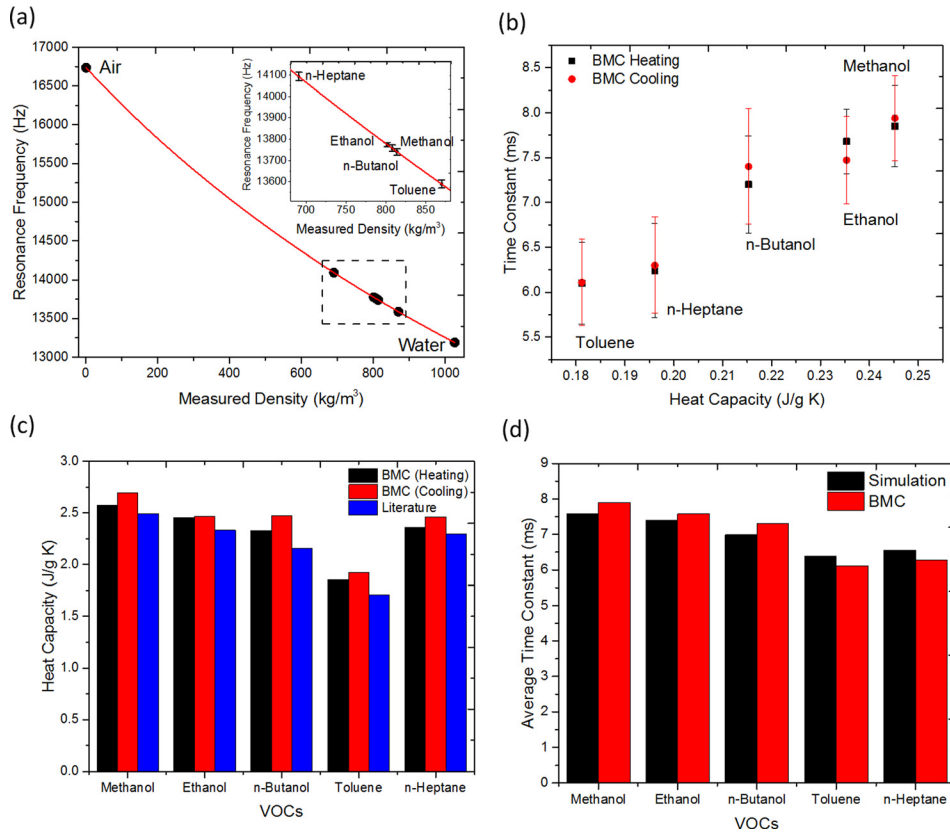


FIG. 3. (a) Resonance frequency of the BMC as a function of the density of samples. (b) Time constant of the BMC plotted against mass weighted average heat capacity of the samples. (c) Extracted heat capacity of the VOCs in comparison with values taken from literature.³⁴ (d) Average time constants (of liquid-filled BMC) determined by experimental data as well as simulations.

$$C_{pl} = C_{pm}/m_R = (\tau/S_C)/\{(\rho_l V_l)/(\rho_l V_l + \rho_{SiN} V_{SiN} + \rho_{Al} V_{Al})\}. \quad (1)$$

Fig. 3(c) provides C_{pl} of the liquids calculated using Equation (1) and the values reported in literature.³⁴ The values of S_C used for heating and cooling cycles are 30 and 31 ms/(J g⁻¹ K⁻¹), respectively. The error between calculated and literature values of C_{pl} range from 3% to 13%. This error is mainly due to the lack of linearity and the error in the data presented in Fig. 3(b). This can be improved by performing measurements in vacuum where heat loss from air convection will be negligible.

A simple one-dimensional conduction based model would suggest that the time constant and heat capacity can be related by $\tau = (L/ka)(\rho C_p V)$. However, in order to take into account the contribution from the system geometry, convective and radiative heat transfers, we performed a two dimensional thermal stress simulation using COMSOL Multiphysics[®]. For the simulation, the heat flux entering the BMC is assumed to be 36% of the radiative flux from the laser with an optical power of 86 mW at an ambient temperature of 25 °C. Coupling of the strain field with the temperature field is obtained by solving the following equations:

$$\rho_l C_{pl} (\partial T / \partial t) = \nabla \cdot (k_l \nabla T), \quad (2)$$

$$\varepsilon_T = \alpha (T - T_{ref}), \quad (3)$$

where δT is temperature gradient, k_l is the thermal conductivity of the VOC samples, ε_T is the thermal strain, α is the coefficient of thermal expansion, and T_{ref} is the reference temperature (set to 293.15 K). A zero-displacement boundary condition on one boundary is used for Equation (3), while

for Equation (2), the convective and radiative heat flux boundary conditions are assumed for all surfaces. A convective heat transfer coefficient (h) of 700 W/(m² K)^{35,36} and a surface emissivity of 0.8 is assumed for the BMC boundary. Equation (3) is used to determine the equilibrium displacement of the cantilever. We have used the material properties selected from literature³⁴ for calculations. Fig. 3(d) presents a good match between the average time constant of the BMC (filled with different samples) and the numerical solution from COMSOL. A near linear trend suggests that with further optimization in the BMC materials and improvements in the experimental setup, it is possible to obtain more accurate data.

We have demonstrated a BMC-based closed chamber micro-calorimeter which is compatible with lab-on-a-chip platforms. It is capable of providing online thermal characterization of small volumes of liquids. Simultaneous measurements of heat capacities and densities of sub-nanoliter volumes of five volatile organic compounds are demonstrated. An optical heating mechanism and the structural material of the BMC allow it to be used for a wide range of liquids, including those which may be corrosive towards metallic heaters in resistive heating based calorimeters. With an average sensitivity of 30.5 ms/(J g⁻¹ K⁻¹) and a resolution of 23 mJ/(g K), the BMC can estimate the heat capacity of a sample in a few milliseconds which is three orders of magnitude faster than values reported in literature.¹⁸ The BMC also measures the density of the liquid with a sensitivity and resolution of 2.8 Hz/(kg m⁻³) and 6.4 kg m⁻³, respectively. Instead of using an expensive QCL, the introduction of low cost IR LEDs (as light sources) would make this technique quite inexpensive to perform thermal measurements of chemicals.

This research work was supported by the Canada Excellence Research Chairs (CERC) Program and by the Basic Science Research Program through the National Research Foundation of Korea (NRF) funded by the Ministry of Science, ICT & Future Planning (NRF-2014R1A2A1A11053283). Additionally, the authors are grateful to Dr. Selvaraj Naicker (Researcher, University of Alberta) for his guidance in preparation of the manuscript.

- ¹M. Mirasoli, M. Guardigli, E. Michelini, and A. Roda, *J. Pharm. Biomed. Anal.* **87**, 36–52 (2014).
- ²S. J. Trietsch, T. Hankemeier, and H. J. van der Linden, *Chemom. Intell. Lab. Syst.* **108**, 64–75 (2011).
- ³S. L. Biswal, D. Raorane, A. Chaiken, H. Birecki, and A. Majumdar, *Anal. Chem.* **78**, 7104–7109 (2006).
- ⁴A. Cooper, *Biophys. Chem.* **115**, 89–97 (2005).
- ⁵T. Buranda, J. Huang, V. H. Perez-Luna, B. Schreyer, L. A. Sklar, and G. P. Lopez, *Anal. Chem.* **74**, 1149–1156 (2002).
- ⁶K. K. Frederick, M. S. Marlow, K. G. Valentine, and A. J. Wand, *Nature* **448**, 325–329 (2007).
- ⁷J. M. Crosthwaite, M. J. Muldoon, J. K. Dixon, J. L. Anderson, and J. F. Brennecke, *J. Chem. Thermodyn.* **37**, 559–568 (2005).
- ⁸J. Lerchner, T. Maskow, and G. Wolf, *Chem. Eng. Process.* **47**, 991–999 (2008).
- ⁹R. E. Gerver and A. E. Herr, *Anal. Chem.* **86**, 10625–10632 (2014).
- ¹⁰W. C. Fon, K. C. Schwab, J. M. Worlock, and M. L. Roukes, *Nano Lett.* **5**, 1968–1971 (2005).
- ¹¹S. Sadat, E. Meyhofer, and P. Reddy, *Appl. Phys. Lett.* **102**, 163110 (2013).
- ¹²B. G. Burke, D. A. LaVan, R. S. Gates, and W. A. Osborn, *Appl. Phys. Lett.* **101**, 243112 (2012).
- ¹³X. C. Zhang, E. B. Myers, J. E. Sader, and M. L. Roukes, *Nano Lett.* **13**, 1528–1534 (2013).
- ¹⁴C. Canetta and A. Narayanaswamy, *Appl. Phys. Lett.* **102**, 103112 (2013).
- ¹⁵B. G. Burke and D. A. LaVan, *Appl. Phys. Lett.* **102**, 021916 (2013).
- ¹⁶J. Varesi, J. Lai, T. Perazzo, Z. Shi, and A. Majumdar, *Appl. Phys. Lett.* **71**, 306–308 (1997).
- ¹⁷G. Zhang, C. Liu, and S. Fan, *Sci. Rep.* **3**, 2549 (2013).
- ¹⁸W. Lee, W. Fon, B. W. Axelrod, and M. L. Roukes, *Proc. Natl. Acad. Sci. U.S.A.* **106**, 15225–15230 (2009).
- ¹⁹J. Xu, R. Reiserer, J. Tellinghuisen, J. P. Wikswo, and F. J. Baudenbacher, *Anal. Chem.* **80**, 2728–2733 (2008).
- ²⁰J. Lerchner, A. Wolf, H.-J. Schneider, F. Mertens, E. Kessler, V. Baier, A. Funfak, M. Nietzsche, and M. Krügel, *Thermochim. Acta* **477**, 48–53 (2008).
- ²¹T. Adrega and A. W. van Herwaarden, *Sens. Actuators, A* **167**, 354–358 (2011).
- ²²B. Wang and Q. Lin, in *2011 IEEE 24th International Conference on Micro Electro Mechanical Systems (MEMS)* (2011), pp. 821–824.
- ²³R. Beigelbeck, H. Nachtebel, F. Kohl, and B. Jakoby, *Meas. Sci. Technol.* **22**, 105407 (2011).
- ²⁴E. B. Chancellor, J. P. Wikswo, F. Baudenbacher, M. Radparvar, and D. Osterman, *Appl. Phys. Lett.* **85**, 2408–2410 (2004).
- ²⁵E. A. Johannessen, J. M. R. Weaver, L. Bourova, P. Svoboda, P. H. Cobbold, and J. M. Cooper, *Anal. Chem.* **74**, 2190–2197 (2002).
- ²⁶M. F. Khan, S. Kim, D. Lee, S. Schmid, A. Boisen, and T. Thundat, *Lab Chip* **14**, 1302–1307 (2014).
- ²⁷S. Olcum, N. Cermak, S. C. Wasserman, K. S. Christine, H. Atsumi, K. R. Payer, W. Shen, J. Lee, A. M. Belcher, S. N. Bhatia, and S. R. Manalis, *Proc. Natl. Acad. Sci. U.S.A.* **111**, 1310–1315 (2014).
- ²⁸I. Lee, K. Park, and J. Lee, *Rev. Sci. Instrum.* **83**, 116106 (2012).
- ²⁹Y. Zhang and S. Tadigadapa, *Biosens. Bioelectron.* **19**, 1733–1743 (2004).
- ³⁰B. Wang and Q. Lin, *Sens. Actuators, B* **180**, 60–65 (2013).
- ³¹M. Khan, S. Schmid, P. E. Larsen, Z. J. Davis, W. Yan, E. H. Stenby, and A. Boisen, *Sens. Actuators, B* **185**, 456–461 (2013).
- ³²D. Lee, S. Kim, and T. Thundat, *Proc. SPIE* **8879**, 88790Q–88790Q (2013).
- ³³See supplementary material at <http://dx.doi.org/10.1063/1.4952614> for additional relevant measurements.
- ³⁴*Ludwig's Applied Process Design for Chemical and Petrochemical Plants*, edited by A. K. Coker, 4th ed. (Gulf Professional Publishing, Boston, 2010), pp. 757–792.
- ³⁵B. Kwon, M. Rosenberger, R. Bhargava, D. G. Cahill, and W. P. King, *Rev. Sci. Instrum.* **83**, 015003 (2012).
- ³⁶M. Toda, T. Ono, F. Liu, and I. Voiculescu, *Rev. Sci. Instrum.* **81**, 055104 (2010).